Princeton Plasma Physics Laboratory

PPPL- 5072

PPPL-5072

Avoidance of Tearing Mode Locking and Disruption with Electro-Magnetic Torque Introduced by Feedback-based Mode Rotation Control in DIII-D and RFX-mod

M. Okabayashi, P. Zanca, E.J. Strait, A.M. Garofalo, J.M. Hanson, Y. In, R.J. La Haye, L. Marrelli, P. Martin, R. Paccagnella, P. Piovesan, C. Piron, L. Piron, D. Shiraki, F.A. Volpe, and the DIII-D and RFX-mod Teams

September 2014

Prepared for the U.S. Department of Energy under Contract DE-AC02-09CH11466.

Princeton Plasma Physics Laboratory
Report Disclaimers

Full Legal Disclaimer

Trademark Disclaimer

PPPL Report Availability

Princeton Plasma Physics Laboratory:

http://www.pppl.gov/techreports.cfm

Office of Scientific and Technical Information (OSTI):

http://www.osti.gov/scitech/

Related Links:

U.S. Department of Energy

Office of Scientific and Technical Information

Avoidance of Tearing Mode Locking and Disruption with Electro-Magnetic Torque Introduced by Feedback-based Mode Rotation Control in DIII-D and RFX-mod

EX/P2-42

M. Okabayashi[1], P. Zanca[2], E.J. Strait[3], A.M. Garofalo[3], J.M. Hanson[4], Y. In[5], R.J. La Haye[3], L. Marrelli[2], P. Martin[2], R. Paccagnella[2], P. Piovesan[2], C. Piron[2], L. Piron[2], D. Shiraki[4,*], F.A. Volpe[4], and the DIII-D and RFX-mod Teams

[1]Princeton Plasma Physics Laboratory, PO Box 451, Princeton, NJ 08543-0451, USA
[2]Consorzio RFX, Associazione Euratom-ENEA sulla Fusione, Padova, Italy
[3]General Atomics, PO Box 85608, San Diego, CA 92186-5608, USA
[4]Columbia University, 2960 Broadway, New York, NY 10027-6900, USA
[5]FAR-TECH, Inc., San Diego, CA 92121-1136, USA
[*]Permanent Address: Oak Ridge National Laboratory, PO Box 2008, Oak Ridge, TN 37831, USA
e-mail contact of main author: mokabaya@pppl.gov

Abstract. Disruptions caused by tearing modes (TMs) are considered to be one of the most critical roadblocks to achieving reliable, steady-state operation of tokamak fusion reactors. Here we have demonstrated a very promising scheme to avoid such disruptions by utilizing the electro-magnetic (EM) torque produced with 3D coils that are available in many tokamaks. In this scheme, the EM torque to the modes is created by a toroidal phase shift between the externally-applied field and the excited TM fields, compensating for the mode momentum loss due to the interaction with the resistive wall and uncorrected error fields. Fine control of torque balance is provided by a feedback scheme. We have explored this approach in two vastly different devices and plasma conditions: DIII-D and RFX-mod operated in tokamak mode. In DIII-D, the plasma target was high β_N plasmas in a non-circular divertor tokamak. In RFX-mod, the plasma was ohmically-heated plasma with ultra-low safety factor in a circular limiter discharge of active feedback coils outside the thick resistive shell. The DIII-D and RFX-mod experiments showed remarkable consistency with theoretical predictions of torque balance. The application to ignition-oriented devices such as International Thermonuclear Experimental Reactor (ITER) would expand the horizon of its operational regime. The internal 3D coil set currently under consideration for edge localized mode suppression in ITER would be well suited to this purpose.

1. Introduction

Over the last few decades, nuclear fusion research has made remarkable progress towards the realization of magnetic fusion reactors. In particular, control capability of plasma configurations and achievability of high plasma pressure in steady-state operation have approached the levels required for ignition-oriented devices, such as International Thermonuclear Experimental Reactor (ITER). Understanding of disruption physics is one of the few remaining challenges for successful tokamak-based reactors. From safe operation view point, it is pre-requsite to develop orderly-controlled paths to avoid releasing several-hundred mega-joules of thermal and magnetic-stored energy. Tearing mode (TM) locking is one of the most common causes of plasma disruptions and occurs in a wide variety of plasma conditions, from low plasma-pressure ohmic discharges to high pressure-neutral beam injection (NBI)-heated plasmas near the ideal MHD stability limit. One approach to avoid this mode locking is to use electro-magnetic (EM) torque by external field coils which compensate for the torque losses of the mode via a feedback scheme. Magnetic field application for disruption control were extensively investigated in the 1990s [1–7] and have revived the attention in combination with electron cyclotron current drive [8]. Recently serious concerns on ITER operational limit and safety of operation have urged us to establish reliable approaches of disruption avoidance.

The application of magnetic feedback is the subject of this paper, jointly explored in two widely differing devices, RFX-mod and DIII-D. In this control scheme, the EM torque to the modes is controlled by a toroidal phase shift between the externally-applied n=1 field and the excited TM fields. Although the proposed approach uses feedback to synchronize the mode, the typical feedback frequency is the order of the inverse of resistive shell time constant, which is of the order of kHz frequencies used in the feedback scheme designed to directly

stabilize the tearing itself. Thus, this scheme is acceptable for practical reactors since the required power is of the order of joule flux loss by the resistive shell. A series of proof-of-principle experiments have been conducted in both devices. Fundamental physics has been established by using models independently developed by RFX-mod and DIII-D groups.

2. Commonalities and Differences of Hardware of RFX-mod and DIII-D

Typical parameters of DIII-D and RFX-mod relevant to this experiment are summarized in Table 1. Some details of commonalities and differences are given below.

Table 1. Typical parameters

	RFX-Mod	DIII-D
Major radius	2.0 m	1.69 m
Minor radius at midplane	0.459	~0.6 m
Plasma shape	Circular	D-shape divertor
Shell, vacuum vessel		
Resistive shell time constant	50 ms (vertical field penetration time) 100 ms for L/R time b/a=1.12	None
Vacuum vessel time constant	3 ms	2–2.5 ms
Typical feedback filtering constant	Not used	10-40 ms
Digital PCS latency	1 ms	0.05 ms
Target plasma	Ohmic low q_{edge}~2.2 plasmas. 2/1Tearing mode	2/1 NTM locking at high beta 2~3, q_{95}=4.5-5.5
Feedback coils location	Outside the shell	Inside shell
Feedback coil numbers	192	12
Feedback sensor for this exp.	B_r sensors inside the shell Inside the resistive shell, but outside the vessel	B_p magnetic sensors inside the shell
Feedback logic	Clean mode control (CMC) Radial B_r flux	Direct mode control with poloidal magnetic pickup

A typical plasma configuration of DIII-D for this experiment uses D-shaped plasmas, with upper single-null divertor with a major radius of 1.66 m, minor radius of 0.6 m, plasma current I_p~1.0–1.2 MA, and toroidal field B_T=1.5–1.8 T. The vacuum vessel serves as a main stabilizing resistive shell against MHD modes. The typical safety factor at the normalized minor radius, ρ, at 95% surface is 4.0–4.5. The feedback coils are located inside the vacuum vessel. The magnetic sensors used in this experiment are poloidal magnetic pickup coils located inside the vacuum vessel [Fig. 1(a)]. The feedback logic is a standard proportional-derivative-integral (PID) control. The feedback system was developed for resistive wall mode (RWM) control [9,10]. The details of I-coil connection for m/n=2/1-mode and feedback logic are discussed in Ref. [10].

In RFX-mod when operated as a tokamak, the typical parameters are I_p~150 kA and B_ϕ~0.55 T. The resistive shell is installed outside the vacuum vessel. The RFX-mod shell is designed to assist high plasma current equilibrium formation of reversed field pinch (RFP) configurations, such as plasma current of I_p~2 MA with B_T=0.55 T to facilitate its MHD stabilization [11–13]. Thus the shell is significantly thick with the resistive time constant of 100 ms, which is much longer than for typical tokamak devices. The feedback coils are located outside the resistive copper shell. The magnetic sensors are between the vacuum-vessel and the stabilizing copper shell [14,15] [Fig. 1(b)]. The feedback is also PID control, as in DIII-D. The feedback made it possible to suppress the m=2, n=1 RWM [16] and to enter routinely at the safety factor $q(a)$<2. In this experiment, $q(a)$ was sustained slightly above 2 in order to explore tearing mode characteristics away from the RWM onset.

3. Modeling of Mode Rotation Control

The fundamental process of the electromagnetic (EM) torque control of mode rotation can be formulated by the torque balance,

$$L\frac{\partial\omega}{\partial t} = L\frac{\omega}{\tau_{loss}} + T_0 + T_{EM} \quad , \tag{3.1}$$

$$T_{EM} = C_{EM}(B_r \delta B_\phi^* + B_r^* \delta B_\phi)) \quad , \tag{3.2}$$

$$C_{EM} = \frac{\pi^2 R_0^2 a}{\mu_0} \quad ,$$

where B_r, the radial field including the field of the mode and the applied feedback radial field, δB_ϕ, the toroidal component of plasma response including the externally applied field, *a,* plasma minor radius, and R_0 is the plasma major radius respectively (the superscript * denotes complex conjugate of these magnetic components). The torque formulation [Eq. (3.2)] is expressed under the large aspect ratio assumption based on a generalized form by R. Fitzpatrick [4]. Here, ω is the mode angular frequency, L is the moment of inertia, T_{EM} is the torque input by the feedback, including the eddy current on the resistive shell, and T_o represents other torque inputs such as by NBI. The τ_{loss} is the momentum loss associated with the momentum coupling to the bulk plasma.

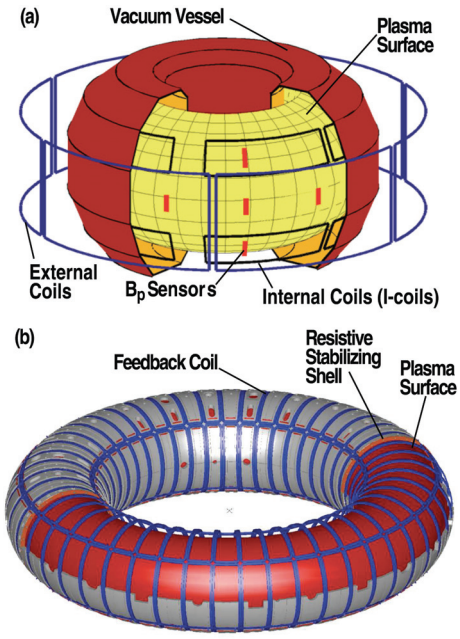

Fig. 1. (a) DIII-D and (b) RFX-mod.

TM locking occurs when strong interaction takes place as the TM amplitude and the eddy current of resistive shell increased in time. Consequently, both TM and bulk plasma rotation were reduced to zero. We present a locking avoidance process using an analytical model with three independent parameters: the field of the mode, feedback field, and magnetic field due to the current induced on resistive shell.

In steady-state conditions, the torque applied, e.g. between input by NBI injection and loss by viscosity balance each other and determine the natural velocity profile, producing the natural mode frequency, ω_0: $0=L\omega_0/\tau_{loss}+T_0$. The EM-torque modifies the mode rotation according to: $0=L(\omega-\omega_0)/\tau_{loss}+T_{EM}$.

Here, we assume that the EM-torque is the dominant effect by neglecting the (small) viscous term. The model we describe is an approximation but captures the essential physical mechanism of the feedback-induced rotation of an otherwise wall-locked tearing mode with uncorrected error field.

With the assumptions discussed above, the equilibrium point of the mode rotation is given by

$$T_{EM}(\omega)=0 \quad . \tag{3.3}$$

The stability at the equilibrium point against small frequency fluctuations is given by

$$dT_{EM}(\omega)/d\omega < 0 \quad . \tag{3.4}$$

The feedback current with the gain G produces the radial field B_r^{FB} to interact the mode,

$$B_r^{FB} = G\delta B_r^{sensor} \qquad G<0 \quad . \tag{2.5}$$

The torque balance [Eq. (3.3)] with the limit of sensor and feedback coils located at the resistive shell (wall) is given by the form $T(\omega)=C_{EM}(f/g)$ [15,17]:

$$f = -(\omega\tau_b)^3(\tau_w/\tau_b) - (\omega\tau_b)(\tau_w/\tau_b) - G\alpha(\omega\tau_b) \tag{3.6}$$

$$g = \left[1+(\omega\tau_b)^2\right]\left[1+(\omega\tau_b)^2(\tau_w/\tau_b)^2\right] \tag{3.7}$$

where τ_b is the band pass time constant of overall feedback system, τ_w is the wall skin time constant, and α is the electro-magnetic coupling coefficient representing the overall coupling between the coil and the plasma. This last term α depends on the geometrical locations of coil and feedback sensor relative to the res*istive shell*.

The torque balance $T(\omega)=0$ [equivalently, $f(\omega)=0$] (2.3) Eq. (3.3) yields a branch with $\omega=0$ and:

two rotating branches: $$\omega\tau_b = \pm\sqrt{\frac{|G_p|}{|G_{p.crit}|}-1} \tag{3.8}$$

where $G_{p.crit}=(\tau_w/\tau_b)/\alpha$ (3.9)

and these rotating branches exist only if $G_p > G_{crit}$.

The stability condition (3.4) $dT(\omega)/d\omega < 0$ (equivalently, $df(\omega)/d\omega < 0$) yields:

$$|Gp| \geq (\tau_b/\tau_W)/\alpha \quad \text{for the two rotating branches} \tag{3.10}$$

$$|Gp| \leq (\tau_b/\tau_W)/\alpha \quad \text{for } \omega=0 \text{ branch} \quad . \tag{3.11}$$

For the $\omega=0$ branch, there is no electromagnetic torque at all. At low gain, the mode of this branch is stable, but at higher gain the torque balance becomes unstable. For the $\omega\neq0$ branches, the stable torque-controlled condition is realized by a torque balance between the torque developed by the feedback currents, so that higher gain requires more torque and hence more current, leading to the deep stable condition as seen in Fig. 2(b).

Further improvement to feedback stability can be attained by applying the feedback field toroidally in a retarded manner, relative to the observed mode location. In this case, the feedback field pushes with a delay from the mode in propagation. Even if some hesitancy appears due to unexpected MHD events or uncorrected error fields, the mode can still be attached stably with the applied field. This forced rotational shift with finite phase shift ϕ_0 can be modeled by torque balance Eq. (3.3) by making the gain complex. The complex gain mixes two rotating-mode branches and a $\omega=0$ branch. The dis-persion relation becomes a fully-cubic form.

The torque balance $T(\omega)=0$ ($f(\omega)=0$) takes the form:

$$f(\omega) = -(\omega\tau_b)^3(\tau_w/\tau_b) - (\omega\tau_b)(\tau_w/\tau_b) + G\sin(\phi_0)\left[1-(\omega\tau_b)^2(\tau_w/\tau_b)\right] - G\alpha\cos(\phi_0)(\omega\tau_b) \tag{3.12}$$

where ϕ_0 is the pre-set value of retarded phase shift. It is to be noted that possible impact with finite phase shift is expected against the unexpected MHD events or uncorrected error fields with low gain operation as seen in Fig. 2 (b).

The condition $f(\omega)=0$ provides the torque balance equilibrium condition $T(\omega)=0$. With $\phi_0=\pi/2$, the Eq. (3.12) $f(\omega)=0$ is identical to Eq. (3.6). It should also be noted that Eq. (3.12) remains intact by switching polarities, $\phi_0 \rightarrow -\phi_0$ together with $\omega \rightarrow -\omega$. Thus, the offset phase shift ϕ_0 determines the mode direction, discussed in further detail in the experimental observations in Sec. 5.

Stability characteristics are shown in Fig. 2**.** The dotted curves are without preset ($\phi_0=0^o$), equivalent to the formula Eq. (3.6). With $\phi_0=30^o$ preset phase shift, the red and green solid curves correspond to stable branches and the blue curve corresponds to one unstable branch of the cubic-ω Eq. (3.12). The phase shift allows the $\omega=0$ branch to lead to stable branch shown by red curve.

For high gain, $|G| >> |G_{crit}| = \{(\tau_w/\tau_b)/\alpha\}$, the system approach finite frequency $\omega\tau_b \sim [G(\tau_b/\tau_w)]^{1/2}$. Finite $\omega\tau_b\neq0$ resulted in the increase of the stability depth of the torque balanced condition. However, stable rotation also occurs without the added phase shift if the gain is larger than G_{crit} as shown in Fig. 2.

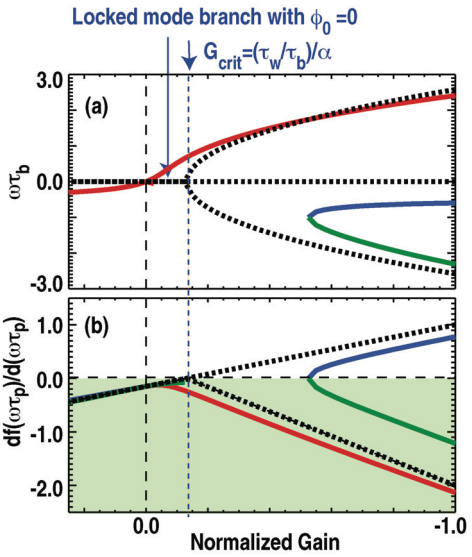

Fig. 2. Model prediction (a) mode rotation frequency normalized by wall time constant vs gain, (b) torque balance stability criterion $dT(\omega)/d\omega < 0$ vs gain. Solid curves are for feedback with an added 30° phase shift, while the dash-curve case has no additional phase shift.

The analytical formulation discussed above indicates that the wall time constant plays a significant role through its ratio to the band-pass time constant for the mode rotation control. In the RFX-mod experiments, the wall time constant was ~40 ms with the bandpass time constant of 10–20 ms, which provides the ratio $\tau_w/\tau_b > 1$. In the DIII-D, the wall time constant was 2–2.5 ms and the bandpass time constant was with 10–50 ms. The ratio is the $\tau_w/\tau_b << 1$. The combination of RFX-mod and DIII-D studies covers wide range of this critical parameter dependence as discussed in the Sec. 5.

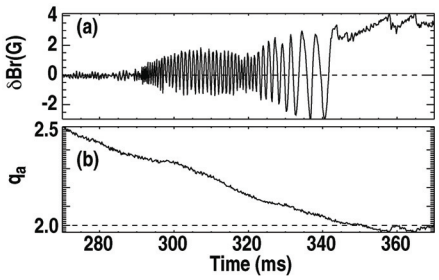

Fig. 3. The excitation of m/n=2/1 mode without feedback (a) 2/1 component of B_r magnetic signal, (b) the q_{edge} in RFX-mod.

4. Demonstrating Feasibility

Near the operational limit of ideal MHD stability, magnetic surfaces begin to tear around rational surfaces, due to the finite resistivity. Most disruptive TMs in the RFX-mod tokamak are excited near the current-driven ideal MHD limit when the safety factor at the plasma surface, q_a, in particular, approaches 2. According to poloidal magnetic pickup probes, the mode structure was identified as m/n=2/1. One example of m/n=2/1 TM in RFX-mod is shown (Fig. 3) with no feedback applied. A TM was excited around q_a~2.3 and gradually increased its amplitude, decreasing the rotation frequency. Locking started just before q_a=2 was reached.

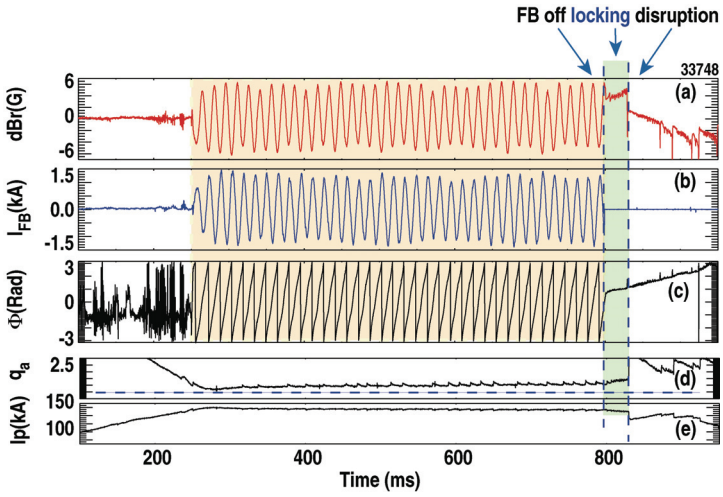

Fig. 4. Long duration of sustainment of m/n=2/1 mode in RFX-mod (a) 2/1 B_r signal, (b) feedback coil current, (c) phase time evolution of the observed 2/1 mode component, (e) the q_{edge} vs time and the plasma current. The TM was controlled by feedback during the time period colored with orange. The mode survived as a locked for a short interval (green).

Feedback could sustain the m/n=2/1 mode rotation (Fig. 4). In this experiment, the feedback was turned on before the TM onset time period without phase offset. With q_a>2 maintained, 1 kA-level of feedback current kept the TM rotating over 0.4 s. The mode waveform was monotonic. After the termination of feedback, locked mode (reflected by the phase becoming nearly constant) was excited, leading to disruption (the sharp drop of the plasma current and B_r signal).

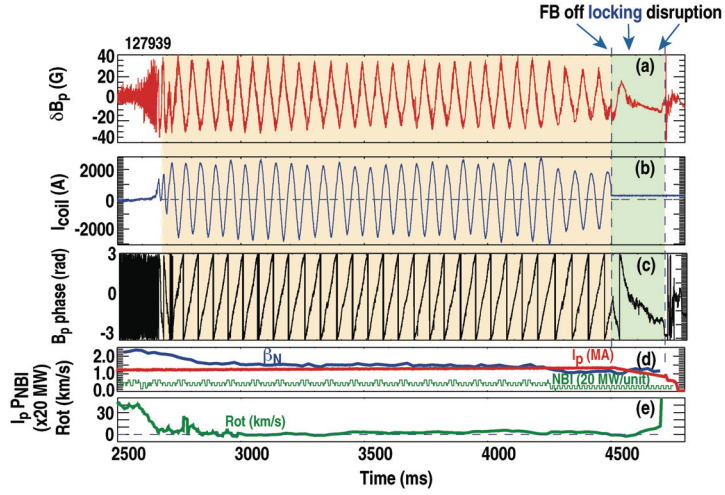

Fig. 5. Long duration of sustainment of m/n=2/1 mode in DIII-D (127939) (a) Time-integrated poloidal magnetic pickup sensor, (b) a feedback coil current, (c) the phase time evolution of m/n=2/1 mode (d) β_N, plasma current I_p and applied NBI power, (e) toroidal plasma rotation near q=2.

For the DIII-D high β_N operation (β_N~2.5), the neoclassical tearing mode (NTM) was excited and without feedback, it led the discharges to disruptions. The feedback with the toroidal forced phase shift ϕ_0=30 deg was applied before the mode was excited (Fig. 5). The feedback kept the

mode rotating at about 17 Hz. The coil current level was about ~2 kA, over a 3 s time interval. The termination of feedback current led to the mode rotation in the reverse direction, disrupting.

5. Consistency of Observation and Modeling in RFX-mod and DIII-D

In this section, we discuss the experimental results of marginal feedback gain in context of the torque balance and operational stability discussion in Sec. 3. As noted earlier, the mode rotation frequency of stable equilibrium point is determined by the gain G, wall time constant τ_w, and band pass time constant τ_b.

5.1 High τ_w/τ_b regime (RFX-mod)

For this RFX-mod tokamak discus-sion, we define Δt to be the latency and K_p the proportional gain defined in a similar manner as in other experiments [15]. The overall coupling coefficient α between the coil and the plasma is represented by the value, α_W with RFX-mod hardware geometry. The overall bandpass time constant τ_b is caused by the latency Δt. The torque balance requirement from Eq. (3.6) is expressed by [15]

$$T_{EM}(\omega) \propto -C^*_{EM}(\omega\Delta t)\left\{(\omega\Delta t)^2 + 1 - \alpha_w(\Delta t/\tau_w)K_p\right\} = 0 \quad . \tag{5.1}$$

The value of $\Delta t = 4$ ms was chosen by considering the latency of the feedback acquisition (≈1 ms) and the coil impedance time for a m/n=2/1 harmonic ($\tau_c \approx 3$ ms). The actual value of α_W was calculated with a large aspect ratio cylindrical model, which is appropriate for circular RFX-mod-tokamak plasmas. The resistive shell time constant, τ_W, is set to 0.1 s. Figure 6 shows the comparison of the experimental results of RFX-mod with the analytical model [Eq. (5.1)] and the results with "RFXlocking" simulation code, originally developed for the TM control in RFX-mod Reversed Field Pinch operation [18].

The minimum gain and the observed frequency are in reasonable agreement. However, the existence of disagreement implies that elements not included in the analytical model are likely responsible. Here, we sought to find additional EM torque causes with RFXlocking code. The RFXlocking code includes the viscous torque and more realistic hardware such as the vacuum vessel (time constant ≈3 ms), the support structure for the coils (time constant ≈24 ms), and more details of feedback system and active coils. These additional resistive elements cause further phase shift between the mode and feedback applied field on the plasma surface. The simulation with only proportional gain K_p (orange squares) should be compared with the analytical model (green curve) since they both have no derivative gain, K_d=0. The addition of K_d (blue points), keeping the ratio K_d/K_p to be twice that of τ_c (τ_c is the coil resistive time constant), simulates the improved dynamic of the current-control circuit of the RFX-mod coils' power supply and makes the RFXlocking simulations more consistent with the RFX-mod experimental condition [16]. In fact, the experimental points (red diamonds) are quite consistent with the results with derivative gain included (blue points). Given the complexity of the RFX-mod layout and feedback system, we cannot expect a perfect agreement between the models and the experiment, but we can say that there is a good qualitative agreement. Thus, we conclude that the observed mode rotation control is consistent with a model based on EM torque balance as we expected.

5.2 Low τ_w/τ_b regime (DIII-D)

In the case of DIII-D, the bandpass filter time constant, τ_b, is explicitly set in the feedback logic as a filtering time constant τ_p. The term α, the coefficient representing the overall EM coupling between the wall and the plasma, is given, with a simple formula at the limit of coil location near the vessel wall radius, $\alpha = (1 + \tau_w/\tau_p)$. With the inclusion of a programmed phase shift ϕ_0, Eq. (3.12) yields,

$$f(\omega) = -\left(\omega\tau_p\right)^3\left(\tau_w/\tau_p\right) - \left(\omega\tau_p\right)\left(\tau_w/\tau_p\right) + G\sin\left(\phi_0\right)\left[1 - \left(\omega\tau_p\right)^2\left(\tau_w/\tau_p\right)\right]$$
$$- G\cos\left(\phi_0\right)\left(\omega\tau_p\right)/\left(1 + \tau_w/\tau_p\right) \quad . \qquad (5.2)$$

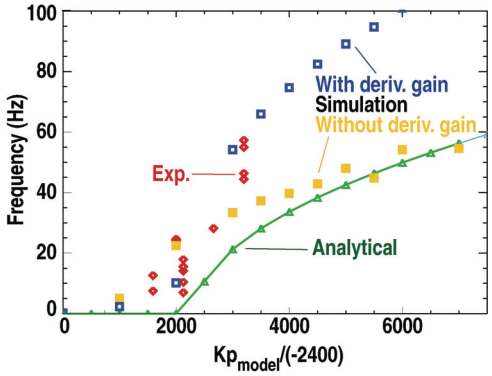

Fig. 6. The comparison of mode rotation frequency and gain in RFX-mod. The data marked with red diamonds are the experimental results. The green solid line is the results with the analytical model [Eq. (5.1)] described in the Sec. 3. Data marked with orange squares are simulations performed with the RFXlocking code with no derivative gain. Data marked with blue squares are RFXlocking code simulations with derivative gain included. The factor of -2400 is a gain convenient for normalization.

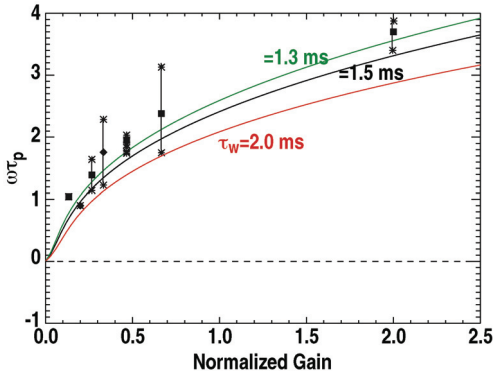

Fig. 7. The observed frequency vs normalized scan. The analytical curves are based on Eq. (5.2) with τ_p = 10 ms.

Figure 7 shows the mode rotation frequency vs normalized gain in DIII-D. The normalization of the gain was based on the RWM studies [19]. The filtering time constant was set 10 ms with the phase shift of 30 deg. The data were obtained by varying gain level with every 100 ms within a shot. The mode prediction was calculated by Eq. (5.2) for τ_w = 2.0, 1.5, and 1.3 ms. The frequency increases as the gain is raised from zero, and then saturates at higher gain, consistent with mode predictions. At low gain, variation in the experimental data may be due to non-uniform rotation correlated with minor internal collapses, while at higher gain levels the mode rotation is more consistent, with greater resilience to internal MHD activity.

The observed frequency is somewhat higher than predicted with τ_w = 2 ms. There are several possible causes. There may exist additional phase shifts not included in the model, such as coil lead inductance, reducing the ratio of τ_w/τ_p. It is also possible that the waveform distortion with lower gain may require additional eignvalues of the wall eddy currents as discussed in Ref. [20]. Since the performance with gain below G_{crit} = 0.2–0.3, where the phase shift is critical, has not been explored yet, the impact of phase shift remains inconclusive.

Nonetheless, overall, the observed dependence is qualitatively in a good agreement with model prediction.

Another example of consistency of the analytical model and experimental observation is shown by the phase shift reversal to the feedback request in the middle of a discharge. The phase of coil current propagation is shown by the three coil currents distributed toroidally [Fig. 8(a)] and the mode and current phases are shown in Fig. 8(b). The solid black line is the phase of current maximum, the dotted line is the current minimum, and the blue line is the mode δB_p. The phase polarity change was requested by feedback from ϕ_0 = -30 deg to +30 deg at 3375 ms. The reversal of the direction of the mode is consistent with the discussion in Sec. 3. The synchronizing δB_p phase relative to the I_{FB} started to change by 180 deg. (solid line matching was shifted to dotted line match after phase reversed). This reflects that the reversed mode rotation requires the switch of δB_px B_r force. The transient time period of direction reversal took ~2–3 ms near the wall time constant, much less than the filtering time constant, τ_p of 10 ms. This is also consistent with the *a priori* hypothesis that torque loss due to the wall finite resistivity plays the dominant role for determining the mode rotation. The observations are consistent qualitatively with the model discussion in Sec. 3.

Overall, RFX-mod and DIII-D experimental results were consistent with simple analytical models. A further-refined model reduced uncertainties in the RFX-mode. The feedback-driven mode rotation control is a robust process represented with a few fundamental parameters.

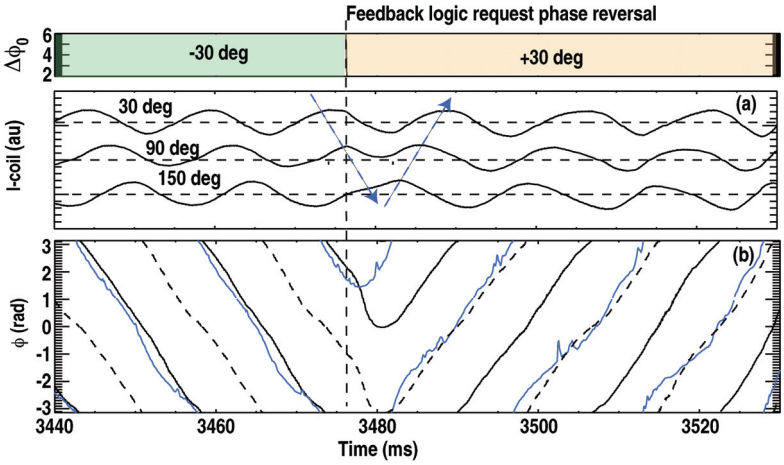

Fig. 8. Switching the $\Delta\phi_0$ pre-setting in the middle of discharge (139605). (a) Current to the coils located at 30°, 90°, 120°, (b) the toroidal phase of coil at 0° (black) and 180° (dotted line) and the mode (blue).

6. Summary

Disruptions caused by tearing modes (TM) are considered to be one of the most critical roadblocks to achieving safe steady state operation of tokamak fusion reactors. Here, a new scheme to avoid such disruptions has been demon-strated by utilizing the electromagnetic (EM) torque produced with 3D coils that are available in many tokamaks. In this scheme, the feedback controls a toroidal phase shift between the externally-applied field and the excited TM fields with feedback and compensates the mode momentum loss due to the interaction with the resistive wall. This concept has been developed in different physics environments. In RFX-mod, the concept was developed through RFP configuration performance optimization. In the DIII-D, the RWM control at high beta exploration and the severe operation limit due to the tearing mode locking have been the driving force for pursuing this approach.

Here, we have demonstrated a proof-of-principle experiment of disruption avoidance due to TM locking by using feedback scheme. In spite of vastly-different plasma condition and hardware arrangement between RFX-mod and DIII-D, it was found that relatively-simple analytical model has provided several essential fundamentals of TM mode rotation control using feedback. The remarkable consistency, although qualitative, of the experimental observations with simple model indicates how robust this process is, thus, encouraging to pursue further. The next step is to explore how to utilize this for orderly-shutdown of hundreds mega joules of thermal and magnetic energy at the onset of TM onset.

This material is based upon work supported in part by the U.S. Department of Energy, Office of Science, Office of Fusion Energy Sciences, using the DIII-D National Fusion Facility, a DOE Office of Science user facility, under Awards DE-FC02-04ER54698, DE-AC02-09CH11466, DE-FG02-04ER54761, DE-FG02-08ER85195, and DE-SC0008520.

References

[1] Morris, A.W., *et al.*, Phys. Rev. Lett. **64**, 1254 (1990).
[2] Hender, T.C., *et al.*, Nucl. Fusion **32**, 2091 (1992).
[3] Jensen, T.H., *et al.*, Phys. Fluids B **5**, 1239 (1993).
[4] Fitzpatrick, R., Phys. Plasmas **6**, 1168 (1999).
[5] Oasa, K., *et al.*, Proc. of 15th IAEA Fusion Energy Conf., Seville, Spain (1995) Vol. 2, p. 279.
[6] Kurita, G., *et al.*, Nucl. Fusion **32**, 1899 (1992).
[7] Navratil, G., *et al.*, Phys. Plasmas **5**, 1855 (1998).
[8] Volpe, F., *et al.*, Phys. Plasmas **16**, 102502 (2009).
[9] Garofalo, A.M., *et al.*, Phys. Plasmas **9**, 4573 (2002).
[10] Okabayashi, M., *et al.*, Nucl. Fusion **45**, 1715 (2005).
[11] Martin, P., *et al.*, Nucl. Fusion **51**, 094023 (2011).
[12] Barana, O., *et al.*, Fusion Eng. Design **71**, 35 (2004).
[13] Manduchi, G., *et al.*, Fusion Eng. Design **87**, 1907 (2014).
[14] Marrelli, L., *et al.*, Plasma Phys. Control. Fusion **49**, B359 (2007).
[15] Zanca, P., *et al.*, Nucl. Fusion **47**, 1425 (2007).
[16] Zanca, P., *et al.*, Plasma Phys. Control. Fusion **54**, 094004 (2012)
[17] Strait, E.J., "Magnetic Control of Magnetohydrodynamic Instabilities in Tokamaks," submitted to Phys. Plasmas (2014)
[18] Zanca, P., Plasma Phys. Control. Fusion **52**, 015006 (2009).
[19] Okabayashi, M., *et al.*, Nucl. Fusion **49**, 125003 (2009).
[20] Chu, M.S. *et al.*, Nucl. Fusion **43**, 441 (2003).

Princeton Plasma Physics Laboratory
Office of Reports and Publications

Managed by
Princeton University

under contract with the
U.S. Department of Energy
(DE-AC02-09CH11466)

P.O. Box 451, Princeton, NJ 08543
Phone: 609-243-2245
Fax: 609-243-2751

E-mail: publications@pppl.gov
Website: http://www.pppl.gov